MODELING THE PHYSICAL, DYNAMICAL, AND CHEMICAL CHARACTERISTICS OF EXTREME EXTRATROPICAL CONVECTION IN THE UPPER TROPOSPHERE AND LOWER STRATOSPHERE

Russell P. Manser[1,2], Cameron R. Homeyer[3], Daniel Phoenix[3]

[1]National Weather Center Research Experiences for Undergraduates Program
Norman, Oklahoma
[2]Saint Cloud State University
Saint Cloud, Minnesota
[3]School of Meteorology, University of Oklahoma
Norman, Oklahoma

ABSTRACT

Stratosphere-troposphere exchange via extreme extratropical convection has implications for climate change. We test the ability of the ARW-WRF model to simulate the physical aspects of a real case of extreme extratropical convection that injected cloud particles into the stratosphere. We find that the model resolves storm structure sufficiently, and proceed to examine the representation of trace gas transport within the same case of convection. Additionally, distributions of trace gas concentrations across the nested model domain are considered in diagnosing irreversible transport. Trace gas transport is seen in model output within the cloud, but little evidence exists for out of cloud transport.

1. INTRODUCTION

The role of convection in stratosphere-troposphere exchange (STE) is not entirely understood, but is an important process that affects the chemistry of the upper troposphere and lower stratosphere (UTLS) and has implications for climate change. We have some observations of the transport of gases via convection (e.g., Fischer et al., 2003, Hegglin et al., 2004, Hanisco et al., 2007, Homeyer et al., 2014a). These observations are difficult to obtain, so modeling becomes essential in our understanding of the physical, chemical, and dynamical relationships between convection and STE. Numerical models have been used to simulate ideal cases of convection that penetrate the tropopause. It is not known if numerical models such as the Advanced Research Weather Research and Forecasting (ARW-WRF) model, are capable of resolving the features associated with a tropopause penetrating supercell. Physical aspects of these storms include gravity wave breaking and lofting of cirrus clouds, as seen in idealized modeling studies (Wang 2003). There are a number of sensitivities to consider in modeling a case such as this. Horizontal grid spacing less than 3 km is required for resolving

Corresponding author address: Russell Manser, Center for Analysis and Prediction of Storms, The University of Oklahoma, National Weather Center, 1200 David L. Boren Blvd., Norman, OK 73072 russell.manser@gmail.com

explicit convection (Weisman et al., 1997). Homeyer (2014) found sensitivities of simulations to vertical grid spacing when resolving convection and the sharpness of the tropopause region. The stability of the lower stratosphere plays a role in the depth of convection into the stratosphere (Homeyer et al., 2014b), thus resolving the UTLS is of importance. Even with these sensitivities considered, it is not known if numerical models can represent the transport of trace gases via convection. Current climate models do not resolve STE via convection due to relatively coarse grid spacing.

The tropopause is a barrier to transport between two chemically distinct layers in the atmosphere: an ozone poor and moist troposphere and an ozone rich and dry stratosphere (Pan et al., 2007). Convection that penetrates the tropopause and causes irreversible mixing in the UTLS results in the transport of water vapor into the lower stratosphere and ozone into the upper troposphere. Greenhouse warming provided by ozone in the troposphere affects the radiation budget when it is nearest the tropopause (Lacis et al., 1990). Additionally, tropospheric ozone has an impact on the respiratory health of ecosystems. Water vapor in the lower stratosphere also acts as a greenhouse gas, further affecting the radiation budget and playing a critical role in the destruction of ozone (Solomon et al., 2010). Convection that initiates within the planetary boundary layer and injects cloud particles into the stratosphere is thought to transport not only those cloud particles,

but also gases such as N_2O, CH_4, CFCs, CO, NO_x, hydrocarbons, and CO_2, which all have an impact on the concentration of ozone in the lower stratosphere (Lacis et al., 1990). Ozone destruction increases exposure to UV radiation at earth's surface.

This study aims to use a numerical model to simulate a real case of convection that reached an altitude of ~20 km based on observed radar reflectivity maximum echo top altitudes. Satellite imagery also reveals an above-anvil cirrus plume. During convection, the transport of three trace gases (ozone, water vapor, and carbon monoxide) will be analyzed in order to determine the role of convection in STE and its chemical impact on the UTLS.

2. MODEL DESIGN AND METHODOLOGY

This study makes use of Advanced Research Weather Research and Forecasting (ARW-WRF) model version 3.7.1 (Skamarock et al., 2008). ARW-WRF is a fully compressible, nonhydrostatic three-dimensional cloud-resolving model. Coupled with chemistry (Grell et al., 2005, Fast et al., 2006), ARW-WRF is capable of simulating the emission, transport, mixing, and chemical transformation of trace gases and aerosols simultaneously with meteorological processes. The model was initialized using a horizontal grid spacing of $\Delta X = 10$ km in the parent domain, with a one-way nested domain of $\Delta X = 2$ km. Weisman et al. (1997) explains that horizontal grid spacing of $\Delta X = 3$ km or finer is necessary in order to explicitly resolve deep moist convection. More recent studies have suggested that a minimum grid spacing of $\Delta X = 250$ m is required to resolve the distribution of reflectivity, cold pool properties, and relative humidity (Bryan and Morrison, 2012). Furthermore, Lane et al. (2005) explain that sensitivities to gravity wave generation exist at finer horizontal resolutions, but gravity waves are still resolved for grids as coarse as $\Delta X = 2$ km. Due to the goals of this study and limited computational resources, we chose a relatively coarse horizontal resolution that would produce gravity waves and explicitly resolve convection within the nested domain (figure 1).

Due to the depth of convection in this case, vertical resolution was given priority over horizontal resolution. Convection penetrated and overshot the lapse rate tropopause, which we define as: "the lowest altitude at which the temperature lapse rate decreases to 2 K km^{-1},

provided that the average lapse rate between this level and all higher levels within 2 km does not exceed 2 K km^{-1}", where the lapse rate, Γ, is defined as the negative of the vertical temperature gradient ($\Gamma = -\partial T/\partial z$; World Meteorological Organization, 1957). Vertical grid spacing of $\Delta Z = 250$ m, with 114 vertical levels, was chosen to resolve convection and the tropopause region properly (Bryan et al., 2003, Homeyer 2015). It has also been found that vertical resolutions coarser than $\Delta Z = 300$ m cause the model to greatly overestimate parcel buoyancy and underestimate the sharpness of the tropopause, resulting in convection that reaches altitudes higher than observed echo top altitudes (Homeyer 2015). Little sensitivity exists in the resolution of gravity waves for vertical grid spacing of $\Delta Z = 400$ m to $\Delta Z = 200$ m (Lane et al. 2005), suggesting that the selected grid spacing of $\Delta Z = 250$ m may be sufficient for the resolution of gravity waves. A model top of 17.5 hPa was set to allow damping to occur within 5 km of the model top without affecting the storm itself.
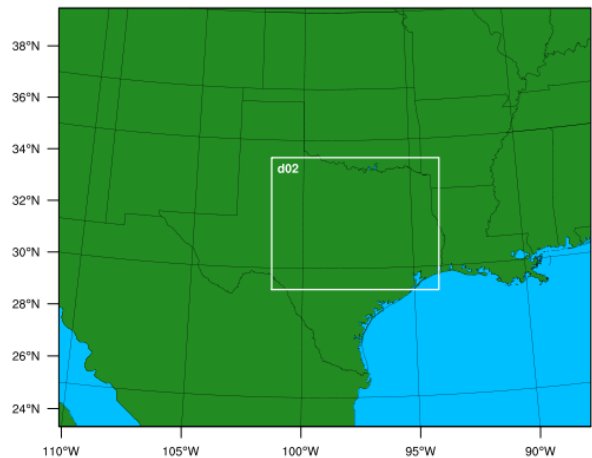

Figure 1: Parent and nested (in white) domains for model initialization with chemistry.

The model was initialized without chemistry for 18 hours starting at 12 UTC May 17, 2013 using boundary conditions obtained from two separate sets of model output. The model was first initialized with ERA-Interim 6-hourly reanalysis output provided by the European Centre for Medium-Range Weather Forecasts (ECMWF). ERA-Interim has a horizontal resolution of ~80 km and a vertical resolution of 650 – 1000 m in the extratropical UTLS. The model was also initialized with 3-hourly model output from the Global

Forecast System (GFS) provided by the National Centers for Environmental Prediction (NCEP). Horizontal resolution is ~27 km across the globe and has 64 vertical layers in a domain from the surface to 0.27 hPa (~55 km). This study does not aim to test sensitivities in the model, so all other previously mentioned model settings, as well as parameters listed below, were held constant for both initializations.

This study makes use of the National Severe Storms Laboratory (NSSL) 2-moment scheme as the bulk microphysics package (Mansell et al. 2010). This package was chosen due to the quality resolution of the physical characteristics of severe storms and the representation of water vapor in the stratosphere (Daniel Phoenix 2016, personal communication). Additional physical parameters specified include the Quasi-normal Scale Elimination (QNSE) for the Planetary Boundary Layer (PBL) scheme (Sukoriansky et al., 2005). Transport of PBL air is important to this case due to the amount of pollutants in this layer of the atmosphere, many of which affect the chemistry of the UTLS. The QNSE scheme ensures that convection initiation occurs at the correct altitude so that transport is represented as realistically as possible. If convection initiation occurs within the free troposphere rather than the PBL, the concentration of many key gases will be underrepresented and results will not reflect the true transport that occurred.

Most chemistry schemes for ARW-WRF treat the trace gases that this study is concerned with (ozone, water vapor, and carbon monoxide) similarly (Cameron Homeyer, personal communication). The choice of Regional Acid Deposition Model (RADM) chemistry (Stockwell et al., 1990) was thus based on its computational efficiency. Biogenic emissions files were generated with the Model of Emissions of Gases and Aerosols from Nature (MEGAN; Guenther et al., 2006). Volcanic ash emissions were neglected. The U.S. National Emissions Inventory (NEI-05) emissions data and program was used for preparation of emissions. Anthropogenic emissions data was prepared using MOZART emissions data. We acknowledge use of the WRF-Chem preprocessor tool {mozbc, fire_emiss, etc.}, provided by the Atmospheric Chemistry Observations and Modeling Lab (ACOM) of NCAR. These utilities were used to create initial and lateral chemical boundary conditions for model input. The model was initialized with

chemistry for 11 hours starting at 12 UTC May 17, 2013. Output was written hourly and a restart file was written for 20 UTC May 17, 2013. Output was written every five minutes for three hours thereafter.

3. CASE DETAILS

The timeframe of convection was 20 UTC May 17 2013 – 02 UTC May 18 2013 in Texas, just south of the Red River bordering Oklahoma in the continental United States. A relatively small supercell initiated south-southwest in central Texas, which is not focused on in this study. Echo top altitudes were viewed using data provided by the Next Generation Weather Radar (NEXRAD) program Weather Surveillance Radar – 1988 Doppler (WSR-88D) network in the contiguous United States (Crum and Alberty 1993). NEXRAD WSR-88D radar composites used in this study were created using the methods outlined in Homeyer (2014) and revised in Homeyer and Kumjian (2015). Observations indicate maximum echo top altitudes of ~20 km (figure 2). An above anvil moisture plume is apparent in Geostationary Observational Environmental Satellite system (GOES) imagery (figure 3). The storm initiated in an environment with over 5000 J kg-1 of surface based Convective Available Potential Energy (CAPE; Storm Prediction Center Severe Weather Event Archive, 2013), providing the storm with sufficient updraft speeds to penetrate the tropopause and lower stratosphere.
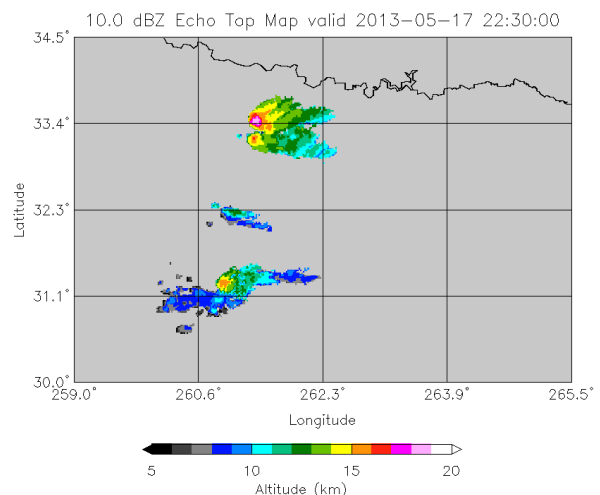

Figure 2: NEXRAD WSR-88D maximum reflectivity echo top altitude (km) observations.
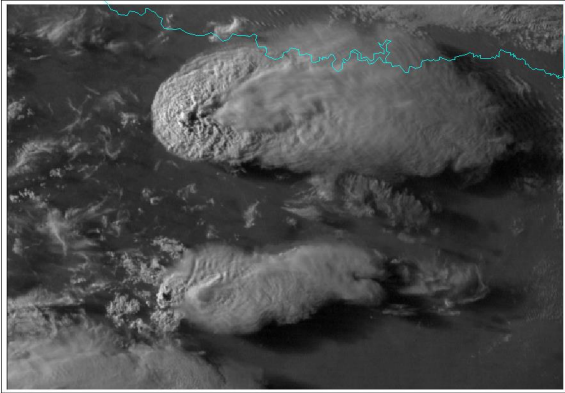
goes13: 20130518T0015Z

Figure 3: observed satellite imagery showing an above-anvil cirrus plume in the northern supercell, which is the focus of this study.

5   8   11   14   17   20
10 dBZ Echo Top Altitude (km)

Figure 4: Model output of maximum reflectivity echo top altitude (km) at May 17, 2150 UTC.

4. RESULTS

Analysis of model output was limited to the nested domain of ΔX = 2 km for both ERA-Interim and GFS initializations. WRF output without chemistry was analyzed for the time period 12 UTC 17 May 2013 – 6 UTC 18 May 2013 at hourly increments. Output from WRF-Chem was analyzed for 20 UTC 17 May 2013 – 2255 UTC 17 May 2013 at 5 minute increments.

4.1 *Model Initialization without Chemistry*

Echo top altitudes were analyzed from model output and compared to observed echo tops from NEXRAD WSR-88D radar data. We found that model initialization with ERA-Interim reanalysis output produced greater and longer lived maximum echo and cloud top altitudes than that with NCEP GFS model output. It is acceptable that the location of convection initiation in model output is further south than the observed location. The goals of this study were more concerned with the model's ability to simulate a physically similar storm, not with the geographical positioning of the storm. Maximum echo top altitudes from model output did not reach the observed altitude of ~20 km (figure 4), however they did exceed the altitude of the tropopause (~14 km) by 2 km, which is high enough for injection of cloud particles into the stratosphere and turbulent mixing of the UTLS to occur. Further support for irreversible transport of gases in the UTLS due to turbulent mixing comes from cloud top altitudes persisting higher than ~14 km to the east of the convective core.
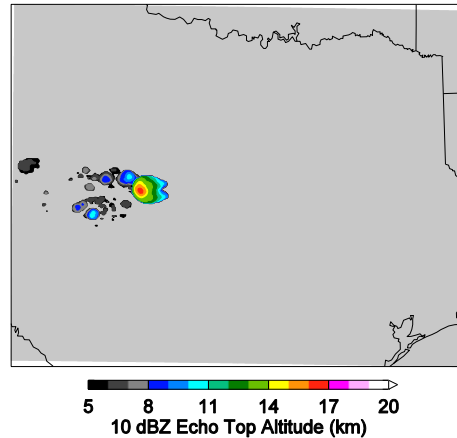
4.2 *Model Initialization Coupled with Chemistry*

The nested domain was shifted south in order to better analyze the storm and its chemical interactions. Intensity, echo top altitude, and cloud top altitude were all conserved when the model was initiated with chemistry (figure 5). An above-anvil cirrus plume is evident from both cloud top altitude and vertical cross-sections of cloud particle concentration (figure 6). Gravity wave breaking is apparent in tightly spaced vertical isentropes above the convective core of the storm (figure 6).

Transport of water vapor and carbon monoxide via convection is clear, and it appears that gravity wave breaking is the mechanism in which stratospheric transport of these gases is irreversible. Wave breaking above the convective core of the storm coincides with enhancements of water vapor and carbon monoxide, but the altitudes at which enhancements occur differ by ~2 km within the model output. Ozone enhancements are not seen in the tropopause region or below. Some downward transport of ozone is seen.

Gases transported within the cloud boundary were represented by the model (figure 7). Mixing of water vapor is evident where enhancements of 80 ppmv are seen next to the convective core of the storm and downstream from the convective core in particular, the latter indicating irreversible transport. Relatively smaller enhancements of 40 ppmv are seen reaching the cloud boundary. Carbon monoxide was irreversibly transported into the stratosphere within the cloud indicated by concentrations of ~100 ppmv near
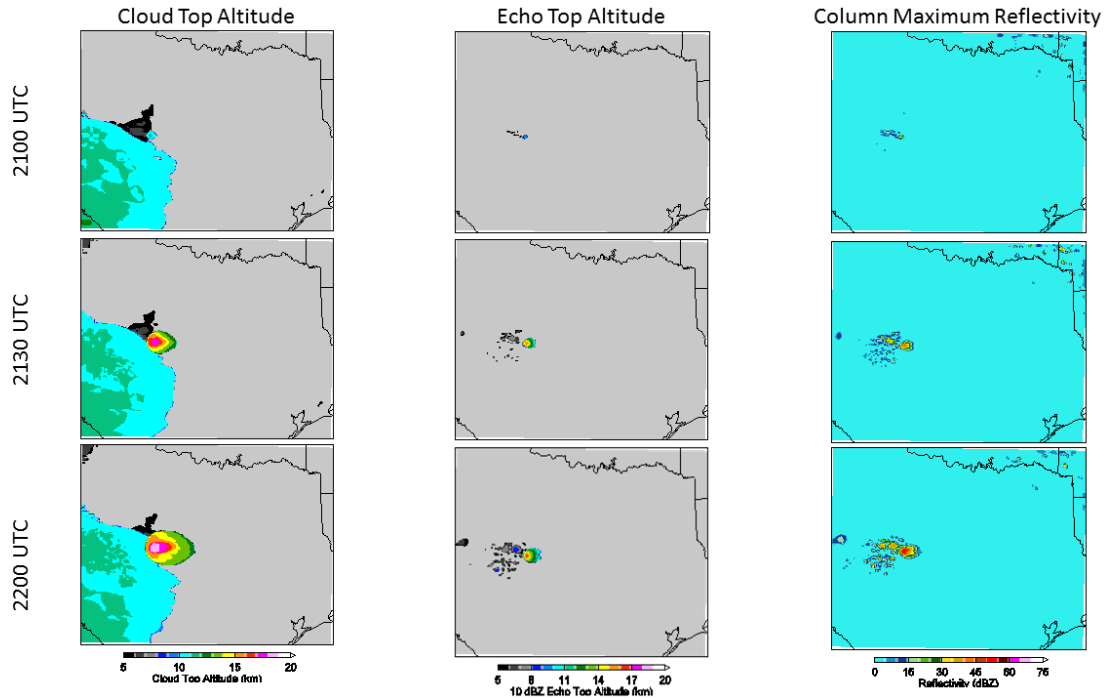
Figure 5: Storm progression shown by model output plots of cloud top altitude in the left column, echo top altitude in the middle column, and column maximum reflectivity in the right column.
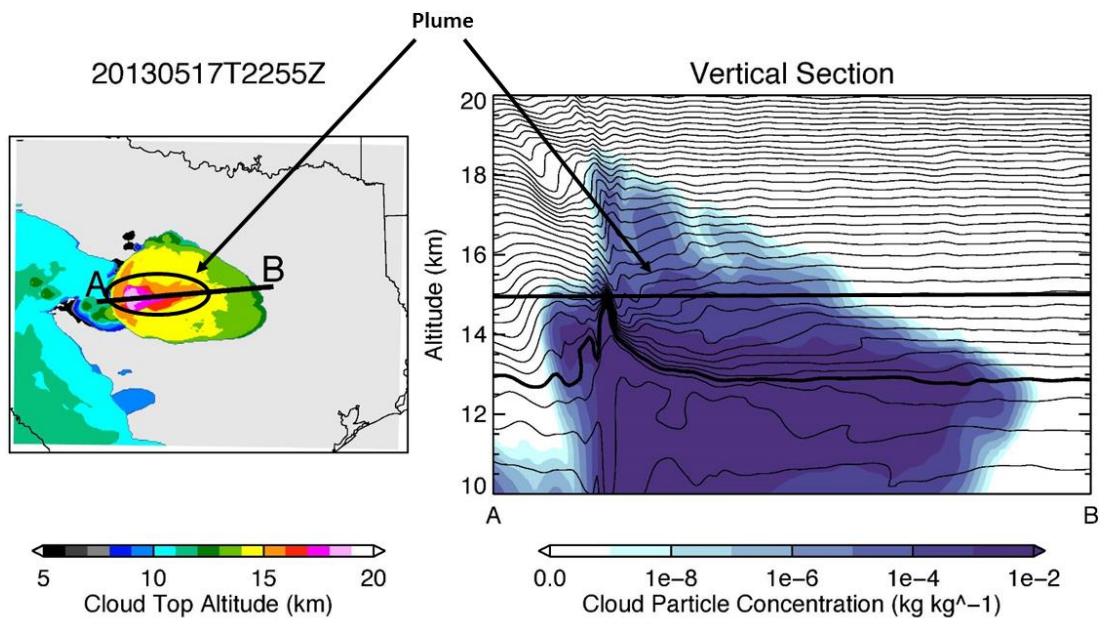

Figure 6: Evidence of an above-anvil cirrus plume is noted by altitude in model output of cloud top altitude (left) and a cross-section of cloud particle concentration (right) corresponding to the line drawn on the left. The cross-section shows potential temperature contours in black, and a bolded contour to indicate the tropopause based on stability. The convective core is apparent where tightly packed vertical potential temperature contours intersect ~15 km.
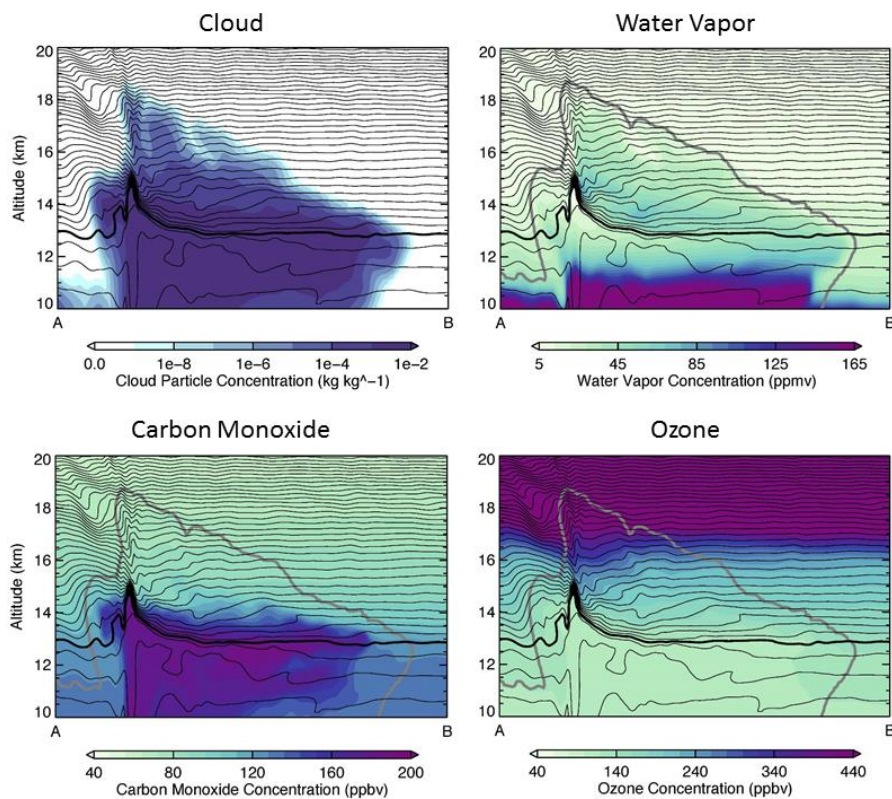
Figure 7: Cross-sections of trace gas concentrations from 10 – 20 km taken from the same model output time and location as in figure 6. The cloud boundary is outlined in gray for water vapor, carbon monoxide, and ozone concentrations.
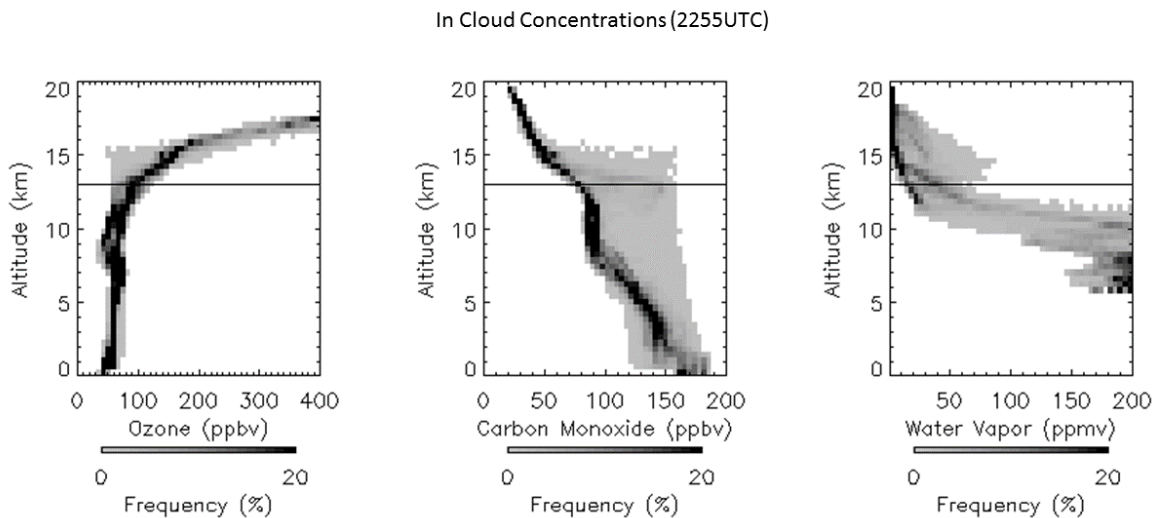
In Cloud Concentrations (2255UTC)

Figure 8: frequency distributions of trace gas concentrations for model output time 2255 UTC. The altitude of the tropopause at this time is denoted by the horizontal line at ~13 km based on stability.

~15 km i.e. no higher than the maximum echo tops altitudes output by the model. Downward transport of ozone occurred close to the convective core, however ozone concentrations below the tropopause did not increase significantly.

Trace gas concentrations were also analyzed across the entire domain. There is clear transport within the cloud, noted by water vapor mixing ratios as high as 80 ppmv and carbon monoxide concentrations in excess of 150 ppmv near 15 km (figure 8). Mixing of ozone within the cloud, above the tropopause, is apparent but there is no evidence of downward transport into the troposphere. There is little to no evidence of out of cloud transport of the three trace gases that were analyzed.

5. CONCLUSIONS AND DISCUSSION

The ARW-WRF model was used to complete a simulation testing the ability of the model to resolve a tropopause-penetrating supercell with an above-anvil cirrus plume. Maximum reflectivity echo top altitudes, cloud top altitudes, and column maximum reflectivity were examined to determine how well the model reproduced the physical characteristics of the storm. It was found that the model was capable of resolving such a storm, so WRF-Chem was used to analyze the chemical impact of the storm on the UTLS. The model replicated the physical aspects of the storm when coupled with chemistry. Cloud top altitudes produced by the model were similar to observed echo top altitudes, though echo top altitudes produced by the model were too low.

Evidence of mixing and irreversible transport were present as indicated by gravity wave breaking coinciding with enhancements of trace gases. Water vapor was lofted to ~19 km, ~5 km above the tropopause. Concentrations were limited to 40 ppmv at the highest altitudes, while higher concentrations of ~80 ppmv were found near and downstream of the convective core. Previous observations have found water vapor mixing ratios of as high as 225 ppmv in the stratosphere as a result of STE via convection (Homeyer et al., 2014a).

The model represented the transport of carbon monoxide up to 2 km above the tropopause. Transport of carbon monoxide was expected to reach the model cloud boundary, but was limited to ~15 km, which is less than the maximum echo top altitude from model output. It is possible that the model is limiting significant transport of carbon monoxide to this height, such that additional mixing as a result of gravity wave breaking cannot extend to deeper altitudes within the overshooting top. The offset related to water vapor and carbon monoxide concentrations in the model should be investigated further.

It is known that gravity wave breaking plays a role in the transport of chemicals in the UTLS during convection that penetrates the tropopause (Wang 2003), but it is unknown if it is essential for significant exchange. It is speculated that gravity wave breaking may not be needed in order for irreversible STE to occur, although there is evidence of frequent wave breaking in this simulation.

The geographical location of the storm in the model may have an effect on the maximum echo top altitude seen in model output. Meteorological conditions at that location in the model may differ from those that were observed. Positioning of convection initiation within ~10 km of the observed storm could produce realistic meteorological conditions in which a better representation of trace gas transport could occur. This study did not examine the reason for why convection initiation, though it is likely due to the placement of surface warming, which was maximized to the north in reality.

Irreversible transport in the UTLS may become more apparent after the storm dissipates, so restarting the model at 2300 UTC and ending after the decay of the storm could help with analyzing transport. Additional observations are needed in order to verify the representativeness of chemistry simulated in the model.

6. ACKNOWLEDGMENTS

7. REFERENCES

Anderson J. G., D. M. Wilmouth, J. B. Smith, and D. S. Sayres, 2012: UV dosage levels in summer: increased risk of ozone loss from

convectively injected water vapor. *Science*, **337**, 835–839.

Bryan, G. H., J. C. Wyngaard, and J. M. Fritsch 2003: Resolution requirements for the simulation of deep moist convection. *Mon. Weather Rev.*, **131**, 2394–2416.

Computational and Information Systems Laboratory, 2012. Yellowstone: IBM iDataPlex System (University Community Computing). Boulder, CO: National Center for Atmospheric Research. http://n2t.net/ark:/85065/d7wd3xhc.

Crum, T. D., and R. L. Alberty, 1993: The WSR-88D and the WSR-88D operational support facility. *Bull. Am. Meteorol. Soc.*, **74**, 1669–1687.

Fast, J. D., W. I. Gustafson Jr., R. C. Easter, R. A. Zaveri, J. C. Barnard, E. G. Chapman, G. A. Grell, and S. E. Peckham, 2006: Evolution of ozone, particulates, and aerosol direct radiative forcing in the vicinity of Houston using a fully coupled meteorology-chemistry-aerosol model. *Journal of Geophysical Research*, **111**, D21305, doi:10.1029/2005JD006721.

Fischer, H., and Coauthors, 2003: Deep convective injection of boundary layer air into the lowermost stratosphere at midlatitudes. *Atmospheric Chemistry and Physics*, **3**, 739–745.

Grell, G. A., S. E. Peckham, R. Schmitz, S. A. McKeen, G. Frost, W. C. Skamarock, B. Eder, 2005: Fully coupled "online" chemistry within the WRF model. *Atmospheric Environment*, **39**, 6957–6975.

Guenther, A., T. Karl, P. Harley, C. Wiedinmyer, P. I. Palmer, and C. Geron, 2006: Estimates of global terrestrial isoprene emissions using MEGAN (Model of Emissions of Gases and Aerosols from Nature). *Atmospheric Chemistry and Physics*, **6**, 3181-3210, doi:10.5194/acp-6-3181-2006.

Hanisco, T. F., and Coauthors, 2007: Observations of deep convective influence on stratospheric water vapor and its isotopic composition. *Geophysical Research Letters*, **34**, L04814, doi:10.1029/2006GL027899.

Hegglin, M. I., and Coauthors, 2004: Tracing troposphere-to-stratosphere transport above a mid-latitude deep convective system. *Atmospheric Chemistry and Physics*, **4**, 741–756, doi:10.5194/acp-4-741-2004.

Homeyer, C. R., 2014: Formation of the enhanced-v infrared cloud top feature from high-resolution three-dimensional radar observations. *J. Atmos. Sci.*, **71**, 332–348, doi:10.1175/JAS-D-13-079.1.

Homeyer, C. R., 2015: Numerical simulations of extratropical tropopause-penetrating convection: Sensitivities to grid resolution. *Journal of Geophysical Research: Atmospheres*, **120**, 7174–7188, doi:10.1002/2015JD023356.

Homeyer, C. R., and M. R. Kumjian 2015: Microphysical characteristics of overshooting convection from polarimetric radar observations. *J. Atmos. Sci.*, **72**, 870–891, doi:10.1175/JAS-D-13-0388.1.

Homeyer, C. R., L. L. Pan, and M. C. Barth, 2014: Transport from convective overshooting of the extratropical tropopause and the role of large-scale lower stratosphere stability. *Journal of Geophysical Research: Atmospheres*, **119**, 2220–2240, doi:10.1002/2013JD020931.

Homeyer, C. R., and Coauthors, 2014: Convective transport of water vapor into the lower stratosphere observed during double tropopause events. *Journal of Geophysical Research: Atmospheres*, **119**, 10941–10958, doi:10.1002/2014JD021485.

Lacis, A. A., D. J. Wuebbles, and J. A. Logan, 1990: Radiative forcing of climate by changes in the vertical distribution of ozone. *Journal of Geophysical Research*, **95**, 9971–9981, doi:10.1029/JD095iD07p09971.

Lane, T.P., and J. C. Knievel, 2005: Some effects of model resolution on simulated gravity waves generated by deep, mesoscale convection. *J. Atmos. Sci.*, **62**, 3408–3419.

Mansell, E. R., C. L. Ziegler, and E. C. Bruning, 2010: Simulated electrification of a small thunderstorm with two-moment bulk

microphysics. *J. Atmos. Sci.*, **67**, 171–194, doi: 10.1175/2009JAS2965.1.

NOAA/NCEP/SPC, 2013: Historic Severe Weather Event Archive. July, 2016, http://www.spc.noaa.gov/archive/index.html

Pan, L. L., and Coauthors, 2007: Chemical behavior of the tropopause observed during the stratosphere-troposphere analyses of regional transport experiment. *Journal of Geophysical Research,* **112**, D18110, doi:10.1029/2007JD008645.

Skamarock, W. C., and Coauthors, 2008: A description of the Advanced Research WRF version 3. NCAR Tech. Note NCAR/TN-475+STR, 113 pp, doi:10.5065/D68S4MVH.

Solomon, S., K. H. Rosenlof, R. W. Portmann, J. S. Daniel, S. M. Davis, T. J. Sanford, and G.-K. Plattner, 2010: Contributions of stratospheric water vapor to decadal changes in the rate of global warming. *Science*, **327**, 1219–1223, doi:10.1126/science.1182488.

Stockwell, W. R., P. Middleton, J. S. Chang, and X. Tang, 1990: The second generation regional acid deposition model chemical mechanism for regional air quality modeling. *Journal of Geophysical Research*, **95**, 16343–16367, doi:10.1029/JD095iD10p16343.

Sukoriansky, S., B. Galperin, and V. Perov, 2005: Application of a new spectral theory of stably stratified turbulence to the atmospheric boundary layer over sea ice. *Boundary-Layer Meteorology*, **117**, 231-257.

Wang, P. K., 2003: Moisture plumes above thunderstorm anvils and their contributions to cross-tropopause transport of water vapor in midlatitudes. *Journal of Geophysical Research*, **108**, 4194, doi:10.1029/2002JD002581.

Weisman, M. L., W. C. Skamarock, and J. B. Klemp, 1997: The resolution dependence of explicitly modeled convective systems. *Mon. Weather Rev.*, **125**, 527–548.

World Meteorological Organization, 1957: Meteorology—A three-dimensional science: Second session of the commission for aerology. *World Meteorological Organization Bulletin*, **4**, 134–138.